Fabrication and Characterization of Porous Metal Emitters for Electrospray Thrusters

IEPC-2007-145

Presented at the 30th International Electric Propulsion Conference, Florence, Italy
September 17-20, 2007

Robert S. Legge Jr.* , Paulo Lozano† and Manuel Martinez-Sanchez‡
Massachusetts Institute of Technology, Cambridge, MA, 02139, USA

Abstract: A repeatable method based on conventional micro fabrication techniques for creating sharpened emitters from porous tungsten has been explored. A laboratory demonstration thruster comprised of 49 of these porous tungsten emitters has been built and tested. The demonstration device operates on the electrostatic field evaporation of ions from ionic liquids. The emitters are contained in three linear emitter arrays which have been shown to support an increase in current of over an order of magnitude when compared to solid cylindrical emitters. Time-of-flight mass spectrometry has be used to show that the emitted beam is purely ionic and is comprised of two species of ions in both positive and negative modes of operation. In addition, thrust measurements conducted on a torsional balance show that the demonstration device is capable of thrusts as high as 5.6 μN at a current of 48 μA and a voltage of 2437 volts for a specific impulse of above 3500 s.

Nomenclature

L = drift distance in the time-of-flight spectrometer
m = particle mass
q = particle electric charge
t = time of flight over drift distance
ϕ_B = on-axis accelerating potential
I_B = electrospray beam current
F = measured thrust

I. Introduction

Traditional colloid thrusters have utilized pressure fed capillary emitter geometry to transport liquid to the base of Taylor cones. This requires pressurization systems onboard the spacecraft which add both mass and complexity to the system. The difficulties in fabricating small, uniform capillaries also pose problems in terms of miniaturization of needle arrays. One way to avoid these issues is to use externally wetted emitter geometries where the liquid is drawn from its reservoir by capillary forces alone. Such passively fed systems supply liquid at the rate established by the electrospray emission process. The use of externally fed emitters in vacuum is possible with ionic liquids. These liquids are molten salts at room temperature and exhibit extremely low vapor pressures. They are formed by positive and negative ions which both can be directly extracted and accelerated to produce thrust when used in bipolar operation.

Since the typical thrust of a single needle operating in the ionic mode is on the order of 0.05 - 0.1 $\frac{\mu N}{\mu A}$, the need to group many needles to produce as much current as possible is essential to increase the domain of applicability of this technology to a variety of different space missions. Based on previous results in our

*Graduate Student, Department of Aeronautics & Astronautics, rlegge@mit.edu
†Assistant Professor, Department of Aeronautics & Astronautics, plozano@mit.edu
‡Professor, Department of Aeronautics & Astronautics, mmart@mit.edu

laboratory, it was found that the emitter geometry and material plays a pivotal role in the amount of current that can be extracted by a single emitter. For instance, it was found that flat ribbon-like configurations yielded considerable more current than traditional cylindrical solid needles.[1]

In this paper we present a method to create flat needle arrays out of porous tungsten substrates using conventional micro fabrication techniques including photolithography and electrochemical etching. These porous flat needles have been shown to emit even more current than a comparably sized solid ribbon emitter. The reason behind this improvement lies in the increased capillary flow capacity provided by the volumetric porosity of the emitter substrate. We go on to construct and characterize a laboratory demonstration thruster comprised of several flat needle arrays to display the technology.

II. Emitter Fabrication

The method of fabrication presented here allows for the creation of single emitters as well as larger emitter arrays. Tungsten emitters were fabricated using electrochemical etching with a polyimide film masking layer. Mask fabrication was carried out at the Microsystems Technology Laboratories (MTL) at MIT while etching was conducted at the Space Propulsion Laboratory at MIT. Figure 1 shows the main steps in the process. First the porous media is filled with photoresist, exposed on both sides with UV light and then developed to create a porous tungsten media with the pores blocked (Step 1). Next a layer of polyimide is added to the front side and is prebaked to drive off solvents (Step 2). Polyimide was chosen as the masking material for its resistance to Sodium Hydroxide[2] and ability to be precisely patterned using standard photolithography techniques. A layer of photoresist is then added on top of the polyimide and is exposed using a transparency mask containing the intended emitter geometry (Step 3). The sample is then developed to remove the exposed parts of the positive photoresist and to etch the underlying polyimide thereby transferring the pattern (Step 4). The photoresist is cleaned off the sample and the polyimide is cured in an oven to harden it against the electrochemical etch chemistry (Step 5). Figures 2a and 2b show the patterened and hardened polyimide on the tungsten. The sample is then electrochemically etched in Sodium Hydroxide until the excess tungsten is removed and the emitter geometry is formed (Step 6). The polyimide is then removed and the emitters are complete.

A. Masking Process Details

The starting material was porous tungsten sheets of 0.25 mm thickness and 2 micron porosity obtained from American Elements, Los Angeles, CA. PI2556 polyimide was purchased from HD Microsystems and photolithography transparencies were obtained from PageWorks, Cambridge, MA. The tungsten sheets were initially cut into 1 cm by 2.5 cm pieces using a Disco Abrasive System Model DAD-2H/6T diesaw and cleaned in acetone followed by isopropanol. A thick layer of Shipley 1827 positive photoresist was then applied to one side of the sheet and allowed to soak into the bulk for 20 s. The sheet was then spun for 60 s starting at 700 rpm and increasing to 1700 rpm with an acceleration of 200 rpm/s The sample was then baked by heating on a hotplate for 20 s at 70°C followed by 30 s in an oven at 90° and 30 s at 130°. Both sides of the sheets were then exposed using a Karl Suss MJB3 for 150 s and then immersed in MF-319 developer until both surfaces are cleared of photoresist. This left photoresist filling the bulk of the porous media to prevent polyimide from entering. The sheets were then cleaned in DI water and dried. Next a 1.5 μm layer of polyimide was spun onto one surface of the tungsten sheet and prebaked using the following protocol. The polyimide was pooled on the surface for 10 s then it was spun at 500 rpm for 5 s and slowly ramped up to 1300 rpm where it was spun for 50 s. The polyimide was then heated on a hotplate at 55° for 30 s and 70° for 30 s followed by oven bakes at 90° for 60 s and 130° for 60 s. The gradual heating protocol employed was designed to limit the amount of holes in the polyimide caused by gas trapped in the bulk of the porous media escaping during rapid heating. Following the prebake, a 5 μm layer of photoresist was spun onto the polyimide and heated at 70° for 30 s on a hotplate and 130° for 90 s in an oven.

The tungsten samples were then exposed for 120 s and developed in MF-319 until the pattern had been transferred to the polyimide. Following development the samples were immersed in acetone for 1 hour in an ultrasonic cleaner to remove the photoresist from the surface and the bulk. The samples were then baked in an anneal furnace to partially cure the polyimide using the following temperature profile. A slow ramp rate from room temperature to 150°C, hold at 150° for 10 minutes then ramp up to 200° and hold for 10 minutes in nitrogen, then a ramp up to 240° and hold for 1.5 hours in nitrogen followed by a slow cool down period.

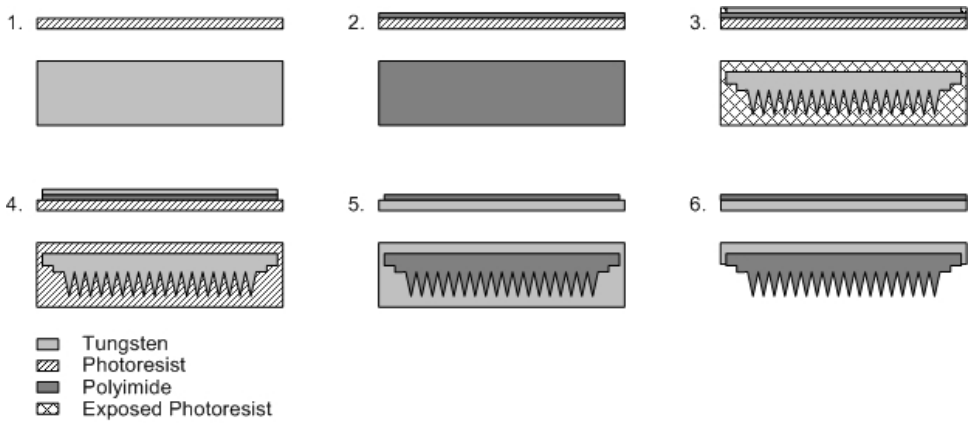

Figure 1. Emitter Fabrication Process Steps

B. Electrochemical Etching

Emitters were prepared from electrochemically etched porous tungsten sheets with a polyimide layer acting as an etch mask. The masked tungsten sheet is placed into a container filled with an etchant solution (1N sodium hydroxide). A DC electric potential is then applied between the tungsten sample and a stainless steel cathode to initiate the etching process. The etching was initially performed in a glass beaker with a circular cathode surrounding the piece. Tips created using this setup were generally uneven with some tips forming significantly faster than others. This is thought to be caused by bubbles forming on the tungsten which inhibits etching in certain areas, and by small eddies that form in the sodium hydroxide directly in front of the tungsten to be etched which adds to the non-uniformities. In addition, a brittle layer is observed to form on the surface of the newly etched tungsten which significantly slows down the etch rate. This is thought to be caused by residual photoresist left in the bulk. To combat these problems several changes to the etching process were made. First, the tungsten is removed periodically and immersed in an ultrasonic cleaner to clear the surface of the residue and to remove bubbles that form on the surface. Second, the etching is carried out in a uniform flow of etchant. This has been shown to reduce the effect of eddies and bubble formation on the etch.[3] Following the completion of the etch, the sodium hydroxide was rinsed off the sample in DI water. The remaining polyimide mask was removed in Piranha[2] (4:1 mixture of sulfuric acid and hydrogen peroxide). Following a rinse in DI water, the emitters were blown dry with nitrogen and were then ready. Figure 2c clearly shows an emitter array during the process of etching. Figure 2d shows a finished emitter with the polyimide masking layer partially removed. Flat emitters with a radius of curvature of $10 - 20\mu m$ in the horizontal direction and $2 - 3\mu m$ in the vertical direction were routinely created as shown in fig 2e and fig 2f.

C. Thruster Design and Fabrication

Since the amount of current, and therefore thrust given by a single emitter is reletively small, there is a need to group many emitters together to form a thruster. A thruster assembly was designed to connect a few emitter sheets together to create a 2D array of emitters. Major design considerations are shown below. The thruster must:

1. Provide precise alignment between the emitter sheets and the extractor grid to reduce beam impingement
2. Provide adaquate insulation (both electrical and fluidic) between the extractor and emitters to reduce the risk of electrical shorting
3. Use materials which are compatible with ionic liquids for long periods of time
4. Allow for easy assembly to reduce the risk of breaking emitters

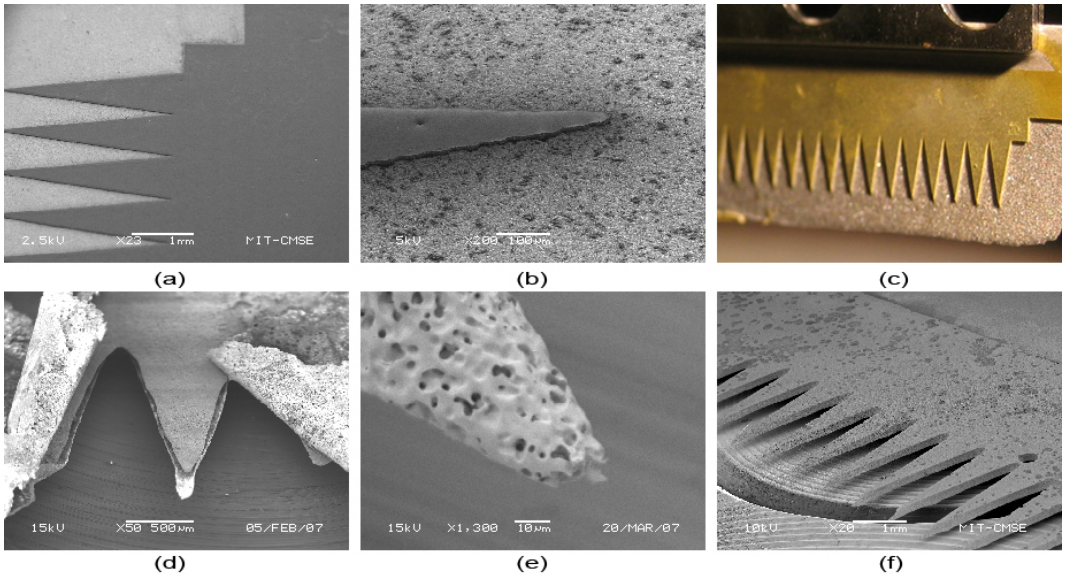

Figure 2. Pictures taken at various stages in emitter fabrication. A polyimide mask was attached and patterned on porous tungsten (a,b). The tungsten was then electrochemically etched (c), the polyimide was removed (d), and flat needle arrays were produced (e,f)

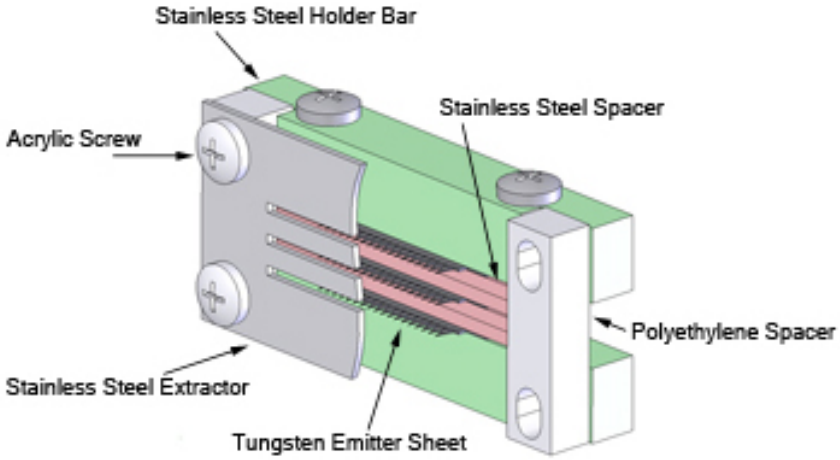

Figure 3. Thruster Design

The design for the thruster is shown in fig 3. The individual emitter sheets are clamped in place between two bars (50 x 7.9 x 7.9 mm stainless steel). Emitter sheet separation is provided by 1.5 mm inch thick stainless steel plates cut by a waterjet. The extractor is made from a 0.635 mm thick stainless steel sheet cut by a waterjet. The individual extractor slits are 1 mm wide which gives clearance for a beam spreading half angle of 51 degrees when the emitter tips are just touching the extractor slit plane. The extractor is attached to the holder bars using two polycarbonate #6-32 screws with two polyethylene spacers. The combination of polycarbonate screws and polyethylene spacers provide electrical insulation between the extractor and emitters and will inhibit the liquid fuel from migrating to the extractor and causing a short. The fabricated thruster is a set of 3 flat needle arrays, each containing up to 18 individual emitters giving a maximum of 54 emitters with a tip to tip separation of 1 mm. The thruster that was tested only had 49 working emitters due to fabrication issues. This gives an emitter density of a little under 0.5 tips per mm^2. The thruster as tested is shown in fig 4 and is approximately 50 x 22 x 10 mm.

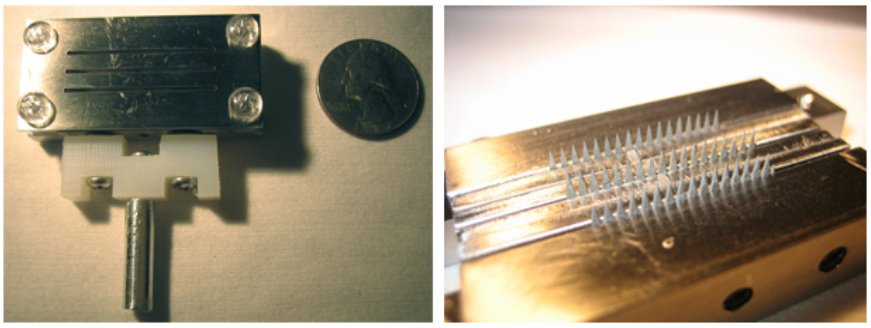

Figure 4. 49 Emitter Electrospray Thruster

III. Thruster Characterization

Ionic liquids such as EMI-BF_4 (3-ethyl-1-methylimidazolium tetrafluoroborate) and EMI-IM (1-ethyl-3-methylimidazolium bis(trifluoromethylsulfonyl)imide) have recently been studied as ionic sources for electrospray applications.[4] These liquids are molten salts at room temperature and have been shown to emit a purely ionic current when exposed to a strong applied potential.[5] They have extremely low vapor pressures which makes them excellent candidates for externally wetted electrospray applications. EMI-BF_4 was chosen for these experiments because of our prior experience with it.

A. Time of Flight

The time-of-flight technique was used to determine the composition of the emitted beam on a single flat needle array containing 6 emitters. The experimental setup is described elsewhere.[6] The time of flight curves for positive (1915.28 V) and negative (-1898.33 V) emission are shown in fig 5. Both graphs show two steps indicating the presence of two distinct ionic species in the beam. From the drift time measured for the particles to travel between the given distance between the electrostatic gate and the detector ($L = 751.57mm$) we can calculate the specific charge ratio and subsequently the mass of the species using Eq. (1). As an approximation, the on-axis accelerating potential is taken to be equal to the extraction potential. In reality it would be up to 7 eV lower.[7] The results are tabulated in table 1.

$$\left(\frac{q}{m}\right)_1 = \frac{(L/t_1)^2}{2\phi_B} \tag{1}$$

In addition we can calculate the contribution of each ion species to the total current by looking at the relative changes in measured current during the time-of-flight tests. The results closely agree with previous time of flight experiments with EMI-BF_4 in both cylindrical needle emitters[6] and with arrays of single flat emitters.[1] The lack of an elongated tail following the steps also indicates that there are no droplets contributing to the emitted current. This is important in that it has been shown earlier that operating an electrospray source in a mixed droplet-ion regime could be very costly in terms of efficiency and specific impulse.[8]

Polarity	**Time of Flight (μs)**	**Mass (amu)**	**% of Total Current**	$\frac{q}{m}$ C/gr	**Corresponding Ion**
Positive	13.9	112.40	42.58	430.6	$[EMI]^+$
(1915.28 V)	22.8	310.15	57.42		$[EMI\text{-}BF_4][EMI]^+$
Negative	12.4	89.49	49.13	513.9	$[BF^-]$
(-1898.33 V)	21.9	287.28	50.87		$[EMI\text{-}BF_4][BF^-]$

Table 1. Emitted Beam Composition.

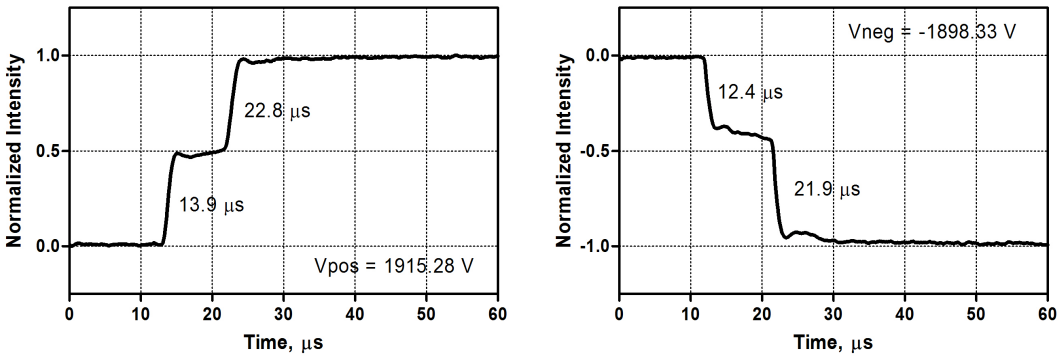

Figure 5. Time-of-flight spectra showing the presence of two families of ions for each polarity.

B. Thrust and Current Measurements

Thrust measurements were conducted at the Busek Company, Natick, MA using a torsional balance capable of measuring sub micro newton forces.[9] The results, shown in fig 5, show that the thruster produced from $0.82\mu N$ to $2.33\mu N$ in the -1282 to -2088 V negative extraction voltage range and from $1.08\mu N$ to $5.67\mu N$ in the 1391 to 2437 V positive extraction voltage range. This corresponds to a thrust per emitter tip of $0.048\mu N$ at -2088 V and $0.116\mu N$ at 2437 V. The leveling off of thrust in the negative mode is potentially due to the thruster approaching the limit of its ability to transport liquid to the tip.

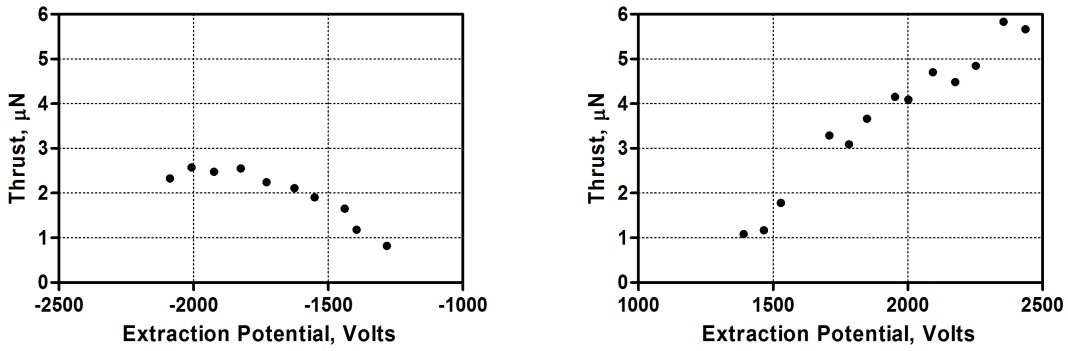

Figure 6. Thrust Produced by a 49 Emitter Thruster

Current as a function of extraction voltage was also monitored. Figure 6 shows the beam current, current leakage to extractor and collected current as a function of extractor voltage. It is seen that a small fraction of the beam current is lost to the extractor which is due to beam impingement. Ideally there would be no current that is lost to the extractor as it is current that is not used for making thrust, and in future designs the extractor geometry may be changed and a better system of alignment will be tested. The beam current was extracted using Eq. (2) from the measrued thrust and the specific charge ratio calculated from the time-of-flight experiements. The results are also plotted in fig 6 and show that the measured beam current is somewhat different than expected. In addition, most noticeably in the positive mode, there is some beam current that is not accounted for in the extractor current and collected current. This is likely due to the effect of secondary electrons caused by the high energy ions hitting the extractor and the collector. These electrons migrate back to the emitters and cause the beam current to be artificially increased. In future tests, the collector will be biased to trap the secondaries and reduce this effect.

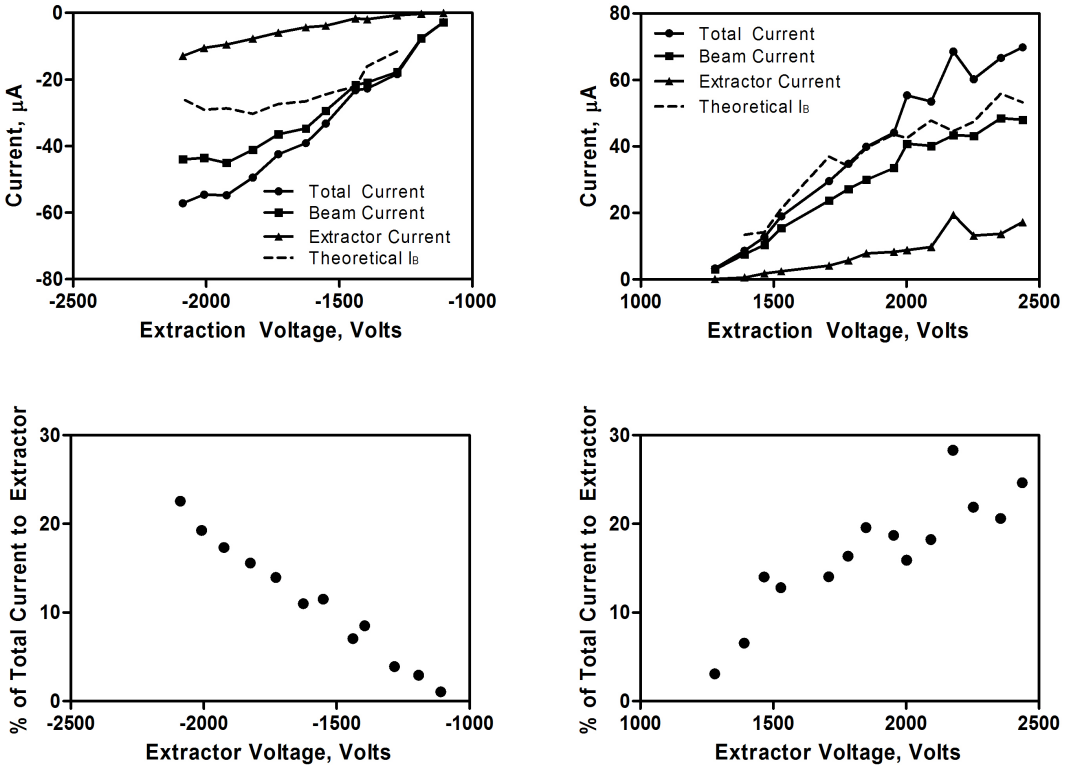

Figure 7. Current vs. Extraction Voltage

$$\frac{F}{I_B} = \sqrt{\frac{2\phi_B}{\left(\overline{q/m}\right)}} \tag{2}$$

IV. Conclusion

A novel fabrication technique has been explored to create sharp porous tungsten emitters suitable for electrospray applications. Additionally, a laboratory demonstration thruster has been designed, built and characterized showing that the emitters can be used successfully for generating thrust using the non-volitile ionic liquid EMI-BF_4. Further work needs to be completed to perfect the fabrication technique in order to create more uniform emitters which will allow for more fluid flow to the emitter tips and subsequently more emitted current per tip. More work also needs to be done in packing the emitters closer together to create denser emitter arrays which would increase the thrust density of the device. The fabrication method presented in this paper allow for emitter spacing much less than the current 1 mm spacing. Along with this is the need for better alignment mechanisms between the emitters and the extractor to reduce the amount of beam impingement on the extractor to increase the efficiency and life of the thruster.

Acknowledgments

Funding for this work was provided by an AFOSR phase II STTR Grant monitored by Mitat Birkan. Also special thanks to Michael McGuirk at Busek for performing the thrust measurements.

References

[1]Lozano, Paulo, B. G. and Martinez-Sanchez, M., "Performance Characteristics of a Linear Ionic Liquid Electrospray Thruster," 29^{th} *International Electric Propulsion Conference*, , No. 192, 2005.

[2]Williams, Kirt R., K. G. and Wasilik, M., "Etch Rates for Micromachining Processes - Part II," *Journal of Microelectromechanical Systems*, Vol. 12, No. 6, December 2003, pp. 761–778.

[3]Landolt, D., "Flow Channel Cell Apparatus for High Rate Electrolysis Studies," *The Review of Scientific Instruments*, Vol. 43, No. 4, April 1972, pp. 592–595.

[4]Romero-Sanz, I., I. A. d. C. and de la Mora, J. F., "Ionic Propulsion Based on Heated Taylor Cones of Ionic Liquids," *Journal of Propulsion and Power*, Vol. 21, No. 2, March-April 2005, pp. 239–242.

[5]Romero-Sanz, I., R. B. M. G.-C. and de la Mora, J. F., "Source of heavy molecular ions based on Taylor cones of ionic liquids operating in the pure ion evaporation regime," *Journal of Applied Physics*, Vol. 94, No. 5, September 2003, pp. 3599–3601.

[6]Lozano, P. and Martinez-Sanchez, M., "Ionic Liquid Ion Sources: characterization of externally wetted emitters," *Journal of Colloid and Interface Science*, , No. 282, 2005, pp. 415–421.

[7]Lozano, P. and Martinez-Sanchez, M., "Efficiency Estimation of EMI-BF_4 Ionic Liquid Electrospray Thrusters," *41st AIAA/ASME/SAE/ASEE Joint Conference and Exhibit*, July 2005.

[8]Lozano, P., "Energy Properties of an EMI-Im ionic liquid ion source," *Journal of Physics D: Applied Physics*, Vol. 39, No. 1, January 2006, pp. 126–134.

[9]Gamero-Castaño, M., "A torsional balance for the characterization of microNewton thrusters," *Review of Scientific Instruments*, Vol. 74, No. 10, October 2003, pp. 4519–4514.